KIAS P11035
HIP-2011-18/TH

Production of two Higgses at the Large Hadron Collider in CP-violating supersymmetry

Priyotosh Bandyopadhyay[a,b1], Katri Huitu [b2]

[a] Korea Institute for Advanced Study,
Hoegiro 87, Dongdaemun-gu, Seoul 130-722, Korea

[b] Department of Physics, University of Helsinki, and Helsinki Institute of Physics,
POB 64, FIN-00014, Gustaf Hällströmin katu 2, Finland

Abstract

Production of two Higgs bosons is studied in the benchmark CP violating supersymmetric scenario (CPX-scenario) at the Large Hadron Collider with $E_{cm} = 14$ TeV. We study the so-called LEP hole area where the experimental bound for the lightest Higgs boson mass can reduce to less than 50 GeV. We analyse the production of the Higgses with decay modes leading to various final state topologies, and consider the dominant Standard Model backgrounds. We find that the hole can be closed with an integrated luminosity of $\sim$100 fb^{-1}, except in special parameter regions, where the production of Higgses gets large enhancement and early data of LHC can cover those regions already at 7 TeV center of mass energy.

[1]priyotosh@kias.re.kr
[2]katri.huitu@helsinki.fi

1 Introduction

CP violation is among the phenomena which are not fully understood in the context of the Standard Model (SM). Although CP violation exists in the SM, and agrees well with the laboratory experiments, there is an inconsistency between the amount of violation and matter content of the Universe, and it is argued that new sources of CP violation are needed.

Many of the proposals for beyond the SM (BSM) physics contain new sources for CP violation. In this work we will consider a supersymmetric model. Many parameters of the model are complex in general, and thus the common choice of real parameters can be thought of as very special. However, general complex parameters lead to the so-called SUSY CP problem, *i.e.* too large violation of CP [1]. In a more complete theory, a suitable amount of CP violation could be explained dynamically. We assume here that such a theory exists.

The physical observables in a general MSSM depend on two types of linearly independent phases [1],

$$Arg[M_i\mu(m_{12}^2)^*],\ Arg[A_f\mu(m_{12}^2)^*].$$

Here M_i, $i = 1, 2, 3$ are the soft gaugino mass parameters, μ is the higgsino mixing parameter, m_{12} is a soft scalar parameter, and A_f are the soft trilinear supersymmetry breaking parameters corresponding to each flavour f. The experimental upper bounds on the electric dipole moments (EDMs) of electrons and neutrons [2, 3] as well as of mercury atoms [4] constrain these phases, which appear also in the Higgs sector of the model via radiative corrections, and they can largely affect both the masses and couplings of the Higgs bosons. It is assumed that the mechanism of the electroweak symmetry breaking manifests itself in any case in the energy range of the LHC. Thus the related particle, the Higgs boson, may be the first one to inform on the BSM physics. If supersymmetry exists, it is indeed very possible that the CP violating effects are shining the Higgs sector.

Search for the Higgs boson(s) is one of the first goals of the Large Hadron Collider (LHC). For the SM Higgs boson, mass bound from the LEP collider is $m_h > 114.4$ GeV [5, 6], and LHC already excludes the SM Higgs boson with masses 145-466 GeV (except 288-296 GeV) at 95% CL []. In the MSSM with real and CP-conserving parameters, the lower limit on the lightest Higgs boson is ~ 90 GeV [8] for any $\tan\beta$. The lower bound on the mass of the lightest Higgs boson of the CP-conserving MSSM from LEP [6] can be drastically reduced or may even entirely vanish if non-zero CP-violating phases are allowed [9, 10]. This can happen through radiative corrections to the Higgs potential, whereby the above mentioned phases of the μ parameter and the A parameters enter into the picture [11, 12]. We will concentrate on such a CP-violating scenario.

The three physical neutral states, which in the CP conserving case have definite CP properties, turn to three neutral states h_i (i=1,2,3) with mixed CP properties. The

collider search limits for all of them are modified since the physical Higgs bosons are mixtures of even and odd degrees of freedom. Due to this mixing through the loop effects, the lightest Higgs boson is almost CP-odd with strongly suppressed coupling to ZZ pair, thus resulting in reduced production rates and consequent weakening of mass limits at collider experiments. The number of parameters in the general MSSM is very large, and thus it is customary to use benchmark points in order to map the relevant phenomenology. In this work we are particularly interested in the possibility that the Higgs boson is light and has not been seen because its couplings are suppressed at LEP. With this in mind we use the so-called CPX model [11, 12] as our benchmark model.

In the CPX scenario the ZZh_1 coupling can be strongly reduced because of the CP violating phases, and the LEP mass limit for the lightest Higgs boson can be lowered to 50 GeV or even less, depending on $\tan\beta$. Thus the LEP searches leave a hole in $(m_{h_1}, \tan\beta)$ parameter space [6]. Complementary channels such as $e^+e^- \to h_1h_2$ suffer also phase space suppression within the hole region. At Tevatron, the CP violation with Higgs production in the SM search channels [13], as well as CP violation specifically through Wh_2 production[14] have been studied.

Within the hole region in addition to ZZh_1 coupling, WWh_1 and tth_1 are suppressed and thus the lightest Higgs boson h_1 is difficult to discover. On the other hand, the relatively heavy neutral Higgs bosons $h_{2,3}$ couple to W, Z and t favourably, but they can decay in non-standard channels, thus requiring a modification in search strategies. So far studies on possible signals of the CPX scenario at the LHC have been restricted to the production of h_i (i=1,2,3) bosons in SM-like channels [15], although all the decay channels have been considered. It has been concluded that parts of the holes in the $m_{H^\pm} - \tan\beta$ or the $m_{h_1} - \tan\beta$ parameter space can be plugged, although considerable portions of the hole, especially for low $\tan\beta$, may escape detection at the LHC even after accumulating 300 fb^{-1} of integrated luminosity.

In [16] the cascade decay of the third generation scalar quarks, mainly $\tilde{t}_1\tilde{t}_1^*$ and $\tilde{b}_1\tilde{b}_1^*$ was explored in the context of Higgs production via charged Higgs decaying to W and Higgs (h_1) bosons and the multi-channel analysis shows that the 'hole' can be probed at an integrated luminosity of 5-10 fb^{-1} assuming $\sqrt{s} = 14$ TeV. It was noted that in a general CP-violating MSSM, the cross section of $\tilde{t}_1\tilde{t}_1^*h_1$ production could be very much larger than that obtained by switching off the CP-violating phases [17]. In [18], it was shown that the associated production of two Higgses could probe the 'LEP hole'. These could be discovery channels, in cases where the t-$\bar{t}$-h_1 and W-W-h_1, Z-Z-h_1 couplings are highly suppressed. In [16, 18] it has been found that although it is possible to probe the 'LEP-hole' in the CPX scenario, in most cases it is difficult to reconstruct all the Higgses (h_1, h_2 and h_3) due to the combinatorial backgrounds from the supersymmetric cascade and production processes. In the context of CP-conserving MSSM, cascade Higgs production has been studied in [19].

The process studied here, namely the Higgs pair production, is a clean channel as

the final state has jets from Higgses only. This gives an extra motivation to look at the pair production channels along with the previously studied ones. We study the production of two Higgs bosons $h_i h_j$ at the LHC, and subsequent decays of the heavy Higgs bosons to Z and the lightest Higgs boson, $h_{2,3} \to Z h_1$, where Z furthermore decays leptonically. It turns out that with an integrated luminosity of 20 fb^{-1} the hole can be covered, except in special parameter regions, where $h_2 h_1$ production gets large enhancement and the required luminosity to cover the relevant parameter region is ≤ 1 fb^{-1}. We study the signal and the Standard Model backgrounds from these production and decay processes, in order to probe the hole region.

We will also point out that in certain benchmark points the two Higgs production through coupling of three Higgs bosons is important, and thus we have a possibility to probe the Higgs potential at those points. Obviously construction of Higgs potential would be of fundamental importance.

The paper is organised as follows. In Section 2 we shortly review the relevant parts of the CPX model, including the resulting Higgs mass spectrum. All of our subsequent numerical analysis are in this framework. In Section 3 we discuss the proposed parton level signal. We do the collider simulation and devise the event selection criteria to reduce the SM backgrounds and present the final numerical results. We also discuss enhancements in the production cross-section for some parameter points. We summarise in Section 4.

2 CPX scenario

As indicated in the introduction, we adopt here the so-called CPX scenario in which the LEP analyses have been performed. In the CPX scenario, it is assumed that certain parameters are related:

$$\begin{aligned} &m_{\tilde{t}} = m_{\tilde{b}} = m_{\tilde{\tau}} = M_{SUSY},\ |A_t| = |A_b| = |A_\tau| = 2M_{SUSY}, \\ &arg(A_t) = arg(A_b) = arg(A_\tau) = 90^0. \end{aligned} \tag{1}$$

It has been observed [11, 12] that the CP-violating quantum effects on the Higgs potential are proportional to $Im(\mu A_t)/M^2_{SUSY}$. The consequences of the CPX scenario have been studied in [20].

The corresponding inputs that we adopt here are compatible with the "hole" left out in the analysis. We take

$$\begin{aligned} &M_{SUSY} = 500\,\text{GeV}, \quad |m_{\tilde{g}}| = 1\,\text{TeV},\ M_2 = 2M_1 = 200\,\text{GeV}, \\ &arg(A_{b,\tau}) = 90^\circ, \quad arg(m_{\tilde{g}}) = 90^\circ,\ \tan\beta = 5 - 10 \end{aligned} \tag{2}$$

where the only difference to the reference [13] lies in a small tweaking in the mass ratio of the $U(1)$ and $SU(2)$ gaugino masses M_1 and M_2, aimed at ensuring gaugino mass

Parameters	BP1	BP2	BP3	BP4
$\tan\beta$	5	5	5	7
ϕ_{A_t}	112	122	124	163
$m_{H^\pm}$	146	155	154	149
m_{h_1}	31.0	30.8	12.6	4.0
m_{h_2}	117.3	124.1	124.2	129.0
m_{h_3}	146.1	152.8	151.5	139.8

Table 1: Benchmark points within the LEP-hole in m_{h_1}-$\tan\beta$ plane and the corresponding neutral Higgs masses.

unification at high scale. It has been checked that this difference does not affect the Higgs production or the decay rates. We vary ϕ_{A_t} to higher values ($\geq 90^\circ$), charged Higgs mass ($m_{H^\pm}$) and $\tan\beta$ to investigate the production of two Higgses. The value of the top quark mass has been taken to be 175 GeV[3]

The first two generation sfermion masses are assumed to be heavy so that the experimental bounds (for example, the electric dipole moment of the neutron) are satisfied. Here we have not considered possible ways of bypassing such bounds, and will set the masses of the first two sfermion families at 10 TeV.

For the collider simulation and analysis to cover the regions of the 'hole', we select benchmark points in the 'hole'. The benchmark points are given in Table 1 with the corresponding neutral Higgs mass spectrum shown with the radiative corrections.

3 Numerical results for the benchmark points

3.1 Production and decay of a h_ih_j pair

As is clear from the Table 1, in the CPX scenario the lightest Higgs mass can be very light. For some parameter points the heavy Higgs bosons ($h_{2,3}$) can decay to the lightest Higgs boson, h_1. We start by analysing the benchmark point BP1 in detail. For BP1 only h_3h_i, i =1,2,3 contributes to the signal we study (*i.e.* jets and opposite sign lepton pair) and thus the signal cross section is the smallest of the chosen benchmark points. For the other benchmark points the analysis will be very similar except for benchmark point 4, where the light Higgs (h_1) is very light ($m_{h_1} \sim 4$ GeV). We give the relevant results for signal and background in the Tables in the next Section.

[3]The central value of m_t has shifted frequently during the years. These shifts change the size of the hole, although the location remains the same. The resulting uncertainty is no bigger than the theoretical uncertainties resulting from the quantum corrections causing the CP violating effects.

$\mathrm{Br}(h_3 \to h_1 Z)$	$\mathrm{Br}(h_3 \to h_1 h_1)$	$\mathrm{Br}(h_2 \to h_1 h_1)$	$\mathrm{Br}(h_2 \to b\bar{b})$	$\mathrm{Br}(h_1 \to b\bar{b})$
0.55	0.11	0.52	0.43	0.93

Table 2: Branching fractions for Higgs bosons in the CPX scenario BP1.

Benchmark point	$\sigma_{h_3 h_i=1,2,3}$ [fb]	$\sigma_{h_1 h_2}$ [fb]
BP1	226	285
BP2	206	323
BP3	248	7929
BP4	464	3119

Table 3: Production cross sections (in fb) for the signal processes at the LHC with $E_{cm} = 14$ TeV in the CPX scenario for the benchmark points.

For the BP1 we list the most important Higgs decay branching ratios in Table 2 . It is seen that $h_3 \to h_1 Z$ branching ratio is large. Since we want to include the opposite sign di-lepton (OSD) in our signal of the event, we consider the process

$$\begin{aligned} pp &\to h_3 h_i, \quad i = 1, 2, 3 \\ &\to h_1 Z h_1 h_1 \text{ or } h_1 Z h_1 \text{ or } h_1 Z b\bar{b} \\ &\to (4b \text{ or } 6b) + OSD \end{aligned} \tag{3}$$

The cross-sections of the Higgs pair production for the benchmark points have been given in Table 3 for E_{cm} =14 TeV. We do not consider lower E_{cm}, since the cross section would be too small to be detected. The cross-sections are computed with `CalcHEP` [21] (interfaced with the program `CPSuperH` [22, 23]). `CTEQ6L` [24, 25] parton distribution functions are used and the renormalization/factorization scale is set to $\sqrt{\hat{s}}$. The largest contribution for the signal in Eq. (3) for benchmark point BP1 comes from $h_3 h_1$ for the Z production. In BP1 h_2 decay to the lightest Higgs boson and Z is not kinematically allowed but, as we will see later, this mode also gets opened up in the case of other benchmark points.

The dominant background from the Standard Model for the signal in Eq. 3 are $t\bar{t}$, $t\bar{t}Z$ and $t\bar{t}b\bar{b}$. In the parton level $t\bar{t}$ seems no to be a background having $2b + OSD + \not{p}_T$ in the final state, but with ISR/FSR the number of jets can increase to a larger value and also due to the large cross-section contributes as one of the dominant backgrounds. Unlike the signal, the invariant mass of leptons will not peak around Z mass. This will help to kill the $t\bar{t}$ backgrounds. Similarly we can also get rid of $t\bar{t}b\bar{b}$. On the other hand $t\bar{t}Z$ could be a true background if both the top quarks decay hadronically. In the

next subsection we simulate both the signal and background through PYTHIA [26] and define the cuts and signal topologies explicitly.

3.2 Signal analysis

In this study, CalcHEP (interfaced to the program CPSuperH) has been used for generating parton-level events for the relevant processes. The standard CalcHEP-PYTHIA interface [27], which uses the SLHA interface [28] was then used to pass the CalcHEP-generated events to PYTHIA [26]. Furthermore, all relevant decay information is generated with CalcHEP and is passed to PYTHIA through the same interface. All these are required since there is no public implementation of CP violating MSSM in PYTHIA. Subsequent decays of the produced particles, hadronization and the collider analyses are done with PYTHIA (version 6.4.22).

We use CTEQ6L parton distribution function (PDF) [24, 25]. In CalcHEP we opted for the lowest order α_s evaluation, which is appropriate for a lowest order PDF like CTEQ6L. The renormalization/factorization scale in CalcHEP is set at $\sqrt{\hat{s}}$. This choice of scale results in a somewhat conservative estimate for the event rates.

In the CPX scenario, although h_1 decays dominantly into $b\bar{b}$, our simulation reveals that in a fairly large fraction of events neither of the b-quarks leads to sufficiently hard jets with reasonable b-tagging efficiency because of the lightness of h_1 in this scenario. To illustrate this, we present in Figure 1 the ordered p_T distributions for the four parton-level b-quarks in the signal from $h_3h_{i=1,2,3}$ and corresponding p_T^{jet} distribution including ISR/FSR. It is clear from this figure that the b-quark which is coming from h_1 has the smallest p_T in a given event, and is often below 40 GeV or thereabout. The other b coming from h_3 or h_2 has larger p_T. For this analysis we have required a b-jet tagging efficiency ($\geq 50\%$) [29].

For hadronic level simulation we have used PYCELL, the toy calorimeter simulation provided in PYTHIA, with the following criteria:

- the calorimeter coverage is $|\eta| < 4.5$ and the segmentation is given by $\Delta\eta \times \Delta\phi = 0.09 \times 0.09$ which resembles a generic LHC detector
- a cone algorithm with $\Delta R = \sqrt{\Delta\eta^2 + \Delta\phi^2} = 0.5$ has been used for jet finding
- $p_{T,min}^{jet} = 20$ GeV and jets are ordered in p_T
- leptons ($\ell = \mathrm{e},\ \mu$) are selected with $p_T \geq 20$ GeV and $|\eta| \leq 2.5$
- no jet should match with a hard lepton in the event

The jet-multiplicity distribution is shown in Figure 2 where the jets are generated using PYCELL. It is evident that the Higgs pair signal has lower jet-multiplicity compared to that of $t\bar{t}$. Thus, jet-multiplicity ($n_{jet} \leq 4$) can reduce the $t\bar{t}$ background considerably.

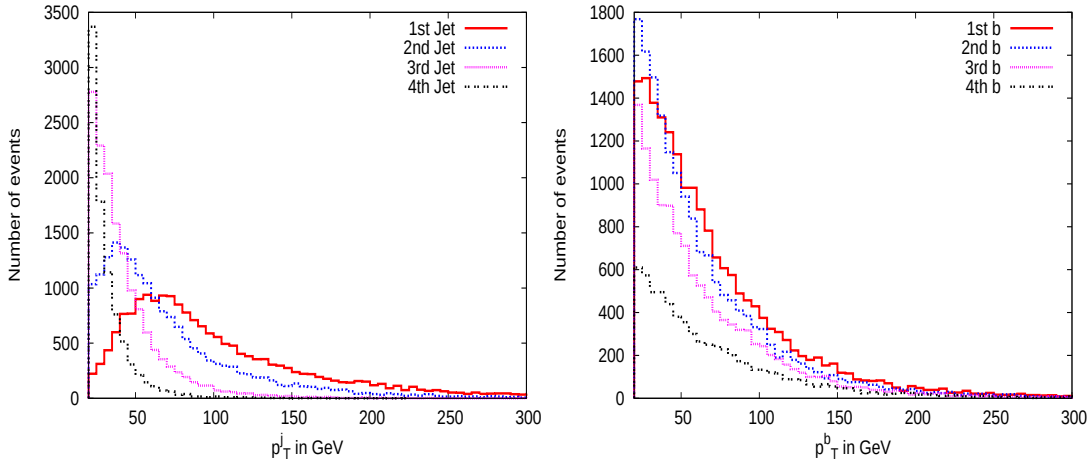

Figure 1: Ordered p_T^{jet} (left) and parton level p_T^b (right) distributions in CPX scenario for $h_3 h_{i=1,2,3}$

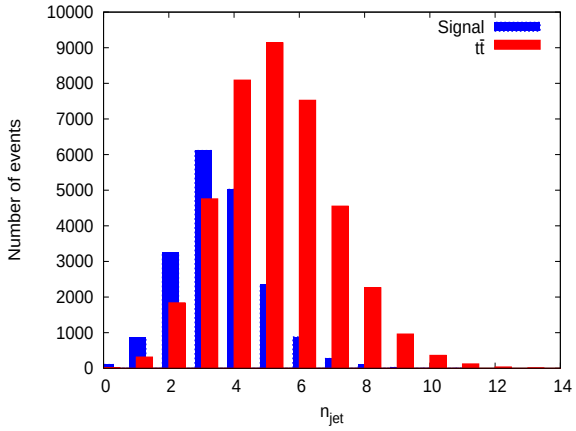

Figure 2: Jet multiplicity distributions in CPX scenario for $h_3 h_{i=1,2,3}$

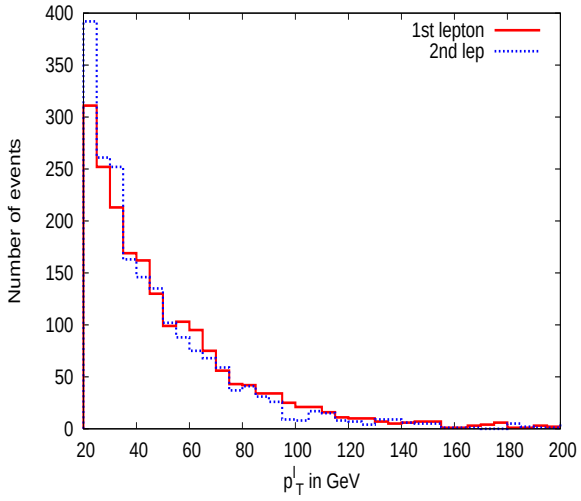

Figure 3: Lepton p_T distributions in CPX scenario for $h_3 h_{i=1,2,3}$

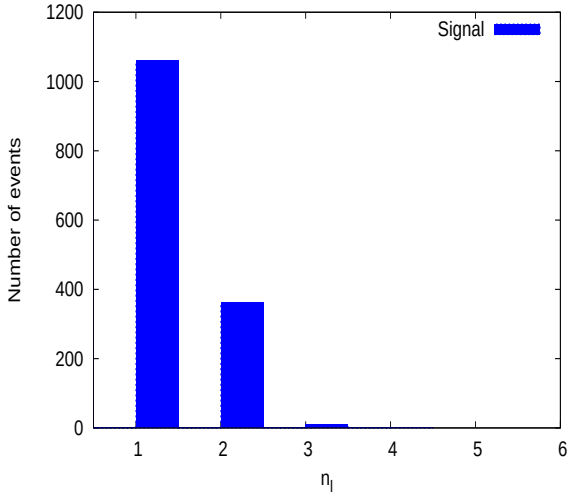

Figure 4: Lepton multiplicity distributions in CPX scenario for $h_3 h_{i=1,2,3}$

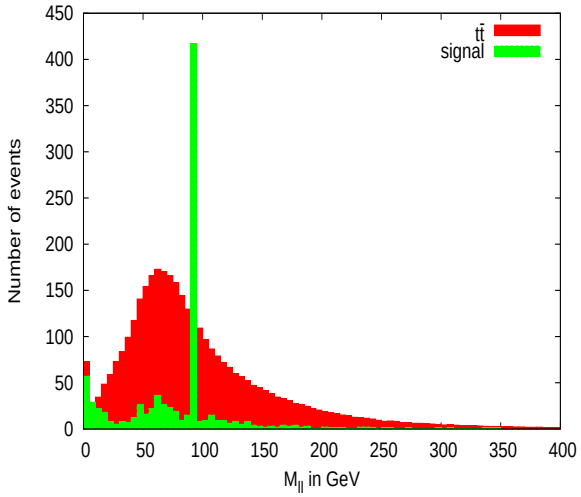

Figure 5: Lepton invariant mass distribution for signal with BP1 in CPX scenario and SM $t\bar{t}$

From Figure 3 we can see the p_T distributions of the leptons where the leptons come from the Z boson which originates from the decay of either h_2 or h_3 via $h_{2,3} \to h_1 Z$. The invariant distribution of these leptons would also peak at the Z mass. This is the best handle to tackle the background like $t\bar{t}$ or $t\bar{t}b\bar{b}$ where the leptons come from two different $W^{\pm}$s from the decays of tops. We also put the isolation criteria on the leptons from jets or leptons as mentioned above. In Figure 4 we plot an isolated lepton multiplicity distribution which shows that there are a few isolated lepton pairs at the end of all the cuts. Figure 5 shows the invariant mass distribution of the isolated leptons for the signal and $t\bar{t}$. For the signal we can reconstruct the Z peak.

Considering all the distributions we have defined five signal topologies with different cuts. Table 4 presents these five different signal topologies and the event numbers at 1 fb^{-1}. The corresponding background events are given in Table 5. Table 6 gives the corresponding significance and required integrated luminosity for 5σ significance. Comparing the signal and backgrounds we can see that for 5σ signal significance we have to achieve at least an integrated luminosity of 108 fb^{-1} for signal 4 of BP1.

Similar analyses for the other benchmark points (BP2 and BP3) for signal and backgrounds are summarised in Tables 4 and 5. In order to achieve 5σ significance for signal 4 of BP2 (Table 6) an integrated luminosity of 84 fb^{-1} is needed. For BP3 the corresponding required luminosity is only 2.5 fb^{-1}. This happens because the cross-sections are enhanced for this benchmark point as shown in Table 3. The huge enhancement is due to the increase in the couplings affecting $h_1 h_2$ cross section, as discussed later.

After calculating the significance we look at the possibility to construct the invariant

No.	Signal topology	BP1	BP2	BP3
1	$n_{jet} \leq 4(b-\text{jet} \geq 3) + l \geq 2(\text{OSD} \geq 1) + \not{p}_T \leq 20$ $p_T^{j_1} \leq 75 + p_T^{j_2} \leq 50 + p_T^{l_1} \leq 90 + p_T^{l_2} \leq 90$ $p_T^{j_3} \leq 40 + M_{eff} \leq 200 + \lvert M_{ll} - 90\rvert \leq 3$	0.27	0.33	9.9
2	$n_{jet} \leq 4(b-\text{jet} = 3) + l \geq 2(\text{OSD} \geq 1) + \not{p}_T \leq 20$ $p_T^{j_1} \leq 90 + p_T^{j_i(i\neq 1)} \leq 70$ $M_{eff} \leq 200 + \lvert M_{ll} - 90\rvert \leq 3 + \phi_{j_2,l_1} \leq 1.6$	0.25	0.30	6.9
3	$n_{jet} \leq 4(b-\text{jet} = 3) + l \geq 2(\text{OSD} \geq 1) + \not{p}_T \leq 20$ $p_T^{j_1} \leq 70 + p_T^{j_2)} \leq 70$ $M_{eff} \leq 200 + \lvert M_{ll} - 90\rvert \leq 2.5 + 0.5 \leq \phi_{j_2,l_1} \leq 1.8$	0.16	0.20	3.9
4	$n_{jet} \leq 4(b-\text{jet} = 3) + l \geq 2(\text{OSD} \geq 1) + \not{p}_T \leq 20$ $p_T^{j_1} \leq 90 + p_T^{j_2)} \leq 70$ $M_{eff} \leq 200 + \lvert M_{ll} - 90\rvert \leq 2.5$	0.31	0.38	10.1
5	$n_{jet} \leq 3(b-\text{jet} = 3) + l \geq 2(\text{OSD} \geq 1) + \not{p}_T \leq 20$ $p_T^{j_1} \leq 75 + p_T^{j_2} \leq 50 + p_T^{j_3} \leq 40$ $+\lvert M_{ll} - 90\rvert \leq 2.5$	0.06	0.08	2.5

Table 4: Event rates for the CPX benchmark points with an integrated luminosity of 1 fb^{-1}

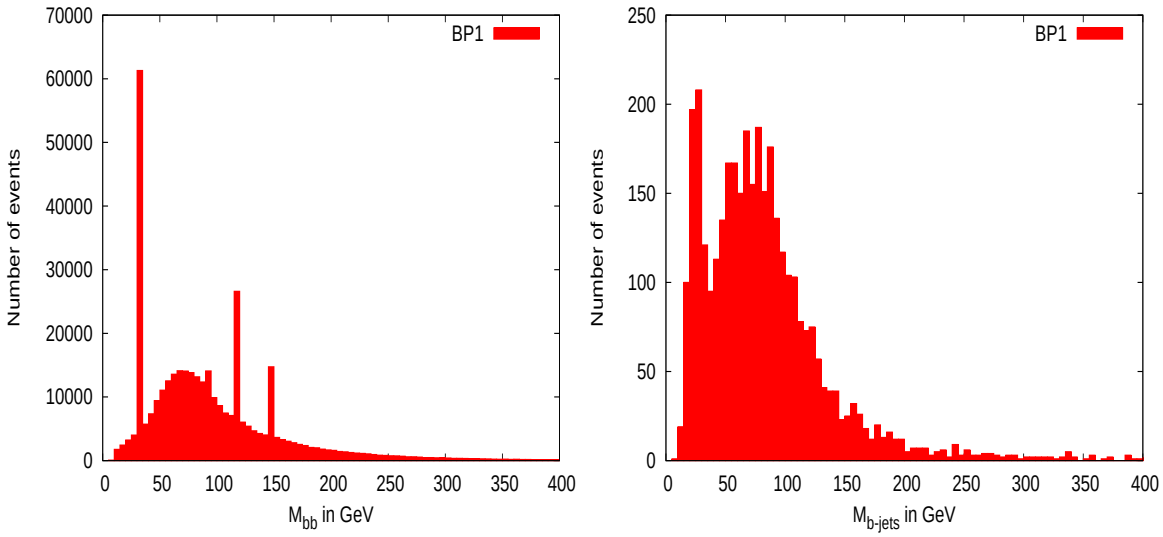

Figure 6: Parton level $b\bar{b}$ invariant mass distribution for signal with BP1 in CPX scenario

No.	Signal topology	$t\bar{t}$	$t\bar{t}Z$	$t\bar{t}b\bar{b}$
1	$n_{jet} \leq 4(b-\text{jet} \geq 3) + l \geq 2(\text{OSD} \geq 1) + \not{p}_T \leq 20$ $p_T^{j_1} \leq 75 + p_T^{j_2} \leq 50 + p_T^{l_1} \leq 90 + p_T^{l_2} \leq 90$ $p_T^{j_3} \leq 40 + M_{eff} \leq 200 + \lvert M_{ll} - 90\rvert \leq 3$	0.10	0.005	0.0
2	$n_{jet} \leq 4(b-\text{jet} = 3) + l \geq 2(\text{OSD} \geq 1) + \not{p}_T \leq 20$ $p_T^{j_1} \leq 90 + p_T^{j_i(i\neq 1)} \leq 70$ $M_{eff} \leq 200 + \lvert M_{ll} - 90\rvert \leq 3 + \phi_{j_2,l_1} \leq 1.6$	0.07	0.004	0.0
3	$n_{jet} \leq 4(b-\text{jet} = 3) + l \geq 2(\text{OSD} \geq 1) + \not{p}_T \leq 20$ $p_T^{j_1} \leq 70 + p_T^{j_2)} \leq 70$ $M_{eff} \leq 200 + \lvert M_{ll} - 90\rvert \leq 2.5 + 0.5 \leq \phi_{j_2,l_1} \leq 1.8$	0.07	0.003	0.0
4	$n_{jet} \leq 4(b-\text{jet} = 3) + l \geq 2(\text{OSD} \geq 1) + \not{p}_T \leq 20$ $p_T^{j_1} \leq 90 + p_T^{j_2)} \leq 70$ $M_{eff} \leq 200 + \lvert M_{ll} - 90\rvert \leq 2.5$	0.10	0.005	0.0
5	$n_{jet} \leq 3(b-\text{jet} = 3) + l \geq 2(\text{OSD} \geq 1) + \not{p}_T \leq 20$ $p_T^{j_1} \leq 75 + p_T^{j_2} \leq 50 + p_T^{j_3} \leq 40$ $+\lvert M_{ll} - 90\rvert \leq 2.5$	0.04	0.001	0.0

Table 5: Event rates for the backgrounds with an integrated luminosity of 1 fb^{-1}

mass peak for h_1. The left part of Figure 6 represents the parton level $b\bar{b}$ invariant mass distribution. From that figure we can see that the peaks corresponding to h_1, Z, h_2 and h_3 are clearly visible. To mimic a more realistic situation, we use the PYCELL jets and require ≥ 4 jets + 2 isolated leptons in the final state. The jet level invariant mass distribution with such a final state topology is shown in the right part of Figure 6. We can clearly see the light Higgs mass peak, i.e., m_{h_1} peak, near 30 GeV. This will remove all the model backgrounds on top of the SM backgrounds. Also we can reconstruct the light Higgs mass (≤ 50 GeV), which is an artifact of the 'CPX' scenario. It has already been noted in the literature that the size and the exact location of the hole in the parameter space depend on the method of calculating the loop correction [30, 31]. However, the calculations agree qualitatively and confirm the presence of the hole.

Since the cross section of the signal for the benchmark point BP3 is much larger than for the other benchmark points, we consider PB3 at LHC with $E_{CM} = 7$ TeV as well. The production cross sections for Higgs pairs are $\sigma(h_1h_2) = 2$ pb and $\sigma(h_1h_3) = 87$ fb. Thus clearly the main contribution for the signals comes from the production of h_1h_2. In Table 7 we present the amount of the signal events for BP3 and the SM background events at $E_{CM} = 7$ TeV and integrated luminosity = 1 fb^{-1}. From the Table one sees that with an integrated luminosity of 6-13 fb^{-1} the significance is 5σ over the SM

Benchmark Points	Signal	Significance at 1fb^{-1}	Required luminosity [fb^{-1}] 5σ significance
BP1	sig1	0.44	129
	sig2	0.44	130
	sig3	0.33	225
	sig4	0.48	108
	sig5	0.19	701
BP2	sig1	0.5	100
	sig2	0.5	103
	sig3	0.4	169
	sig4	0.5	84
	sig5	0.2	473
BP3	sig1	3.1	2.6
	sig2	2.6	3.7
	sig3	2.0	6.5
	sig4	3.2	2.5
	sig5	1.6	10.2

Table 6: Significance at 1 fb^{-1} and the required luminosity for 5σ significance.

		Signal	Background			Required luminosity in fb^{-1}
No.	Final State	BP3	$t\bar{t}$	$t\bar{t}Z$	$t\bar{t}b\bar{b}$	for 5σ Signi -ficance
1	$n_{jet} \leq 4(b-\text{jet} \geq 3) + l \geq 2(\text{OSD} \geq 1) + \not{p}_{\text{T}} \leq 20$ $p_T^{j_1} \leq 75 + p_T^{j_2} \leq 50 + p_T^{l_1} \leq 90 + p_T^{l_2} \leq 90$ $p_T^{j_3} \leq 40 + M_{eff} \leq 200 + \lvert M_{ll} - 90\rvert \leq 3$	3.67	0.026	0.0	0.0	6.9
2	$n_{jet} \leq 4(b-\text{jet} = 3) + l \geq 2(\text{OSD} \geq 1) + \not{p}_{\text{T}} \leq 20$ $p_T^{j_1} \leq 90 + p_T^{j_i(i\neq 1)} \leq 70$ $M_{eff} \leq 200 + \lvert M_{ll} - 90\rvert \leq 3 + \phi_{j_2,l_1} \leq 1.6$	2.46	0.026	0.0	0.0	10.3
3	$n_{jet} \leq 4(b-\text{jet} = 3) + l \geq 2(\text{OSD} \geq 1) + \not{p}_{\text{T}} \leq 20$ $p_T^{j_1} \leq 70 + p_T^{j_2)} \leq 70$ $M_{eff} \leq 200 + \lvert M_{ll} - 90\rvert \leq 2.5 + 0.5 \leq \phi_{j_2,l_1} \leq 1.8$	1.99	0.0	0.0	0.0	12.6
4	$n_{jet} \leq 4(b-\text{jet} = 3) + l \geq 2(\text{OSD} \geq 1) + \not{p}_{\text{T}} \leq 20$ $p_T^{j_1} \leq 90 + p_T^{j_2)} \leq 70$ $M_{eff} \leq 200 + \lvert M_{ll} - 90\rvert \leq 2.5$	3.67	0.052	0.0	0.0	6.9
5	$n_{jet} \leq 3(b-\text{jet} = 3) + l \geq 2(\text{OSD} \geq 1) + \not{p}_{\text{T}} \leq 20$ $p_T^{j_1} \leq 75 + p_T^{j_2} \leq 50 + p_T^{j_3} \leq 40$ $+\lvert M_{ll} - 90\rvert \leq 2.5$	0.80	0.013	0.0	0.0	5.6

Table 7: Event rates for the backgrounds with an integrated luminosity of 1 fb^{-1} at the LHC for ECM=7 TeV.

backgrounds for all the final states.

The scenario for benchmark point BP4 is a little different, as the lightest neutral Higgs (h_1) mostly decays to tau pairs (BR($h_1 \to \tau\tau$) $\sim 90\%$). Thus the search mode for Higgs as well as the final state consist of taus. As in the previous case, the heavier Higgses ($h_{2,3}$) also decay to Z and h_1. The final state then consists of four τs and two opposite sign leptons, invariant mass for which peaks around Z mass. The τs coming from h_1 can be very soft as h_1 in this case is very light (~ 4 GeV, see Table 1). Boost of the light Higgs (h_1) of course increases the p_T of τs from decays. Figure 7 shows the p_T distribution of the partonic τ coming from h_1 which establishes the fact that indeed there are some boosted τs, tagging of which might be possible.

Taus coming from Higgs then decay to pions through one prong or three prong decay. In the present study, we would be using the one prong (one charged track) hadronic decays of the τ-leptons which have a collective branching fraction of about

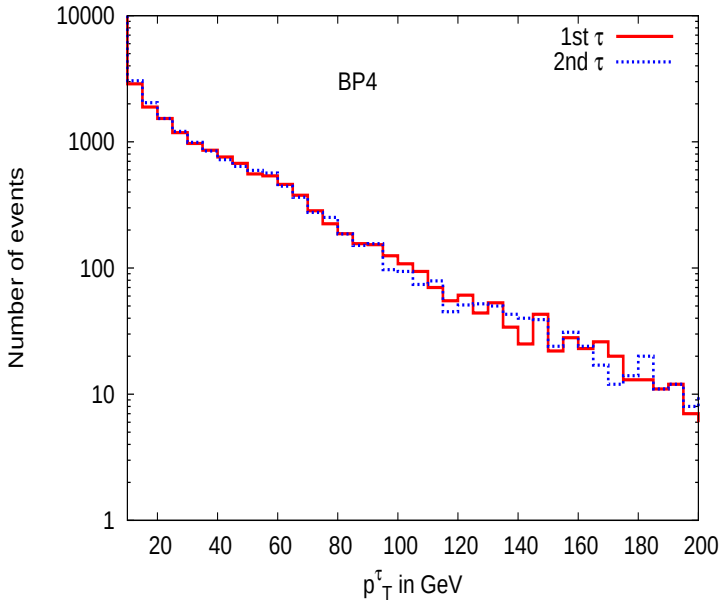

Figure 7: p_T distribution of partonic τ coming from h_1 for BP4.

50% of which almost 90% is comprised of final states with $\pi^{\pm}$, ρ and a_1 mesons. To establish a jet as a τ-jet we take the following approach. We first check, for each jet coming out of PYCELL within $|\eta| \leq 2.5$, if there is a partonic τ within a cone of $\Delta R \leq 0.4$ about the jet-axis. If there is one, then we further ensure that there is a single charged track within a cone of $\Delta R \leq 0.1$ of the same jet axis. This marks a narrow jet character of a τ-jet. Of course there is an efficiency associated to such kind of a geometric requirement which is a function of p_T of the concerned jet and has been demonstrated in the literature [32, 33]. We closely reproduce the values of the τ-tagging efficiencies for the p_T range we adopted for the concerned jets as indicated in references.

Tau tagging efficiency thus decreases when one tries to tag more τ-jets. We optimize our signal with 4-jets among which three are reconstructed τ-jets with one charged track and two opposite sign leptons peak around Z mass. From the event numbers given below, we can see that $\not{p}_T \leq 20$ GeV cut is not necessary as the signal is background free without that as well. Unlike the previous three benchmark points, here only $t\bar{t}Z$ is the possible dominant background that can give two potential τs from the two $W^{\pm}$s coming from the top and another from some jet faking as τ-jet. One can see from Table 8 that the background is zero and the signal has roughly two events at 1 fb^{-1} of integrated luminosity without the missing p_T cut which further reduces the number of signal events. Both of the final states are background free and have a reach with relatively small integrated luminosity.

For benchmark points BP3 and BP4 the total cross-section gets an enhancement

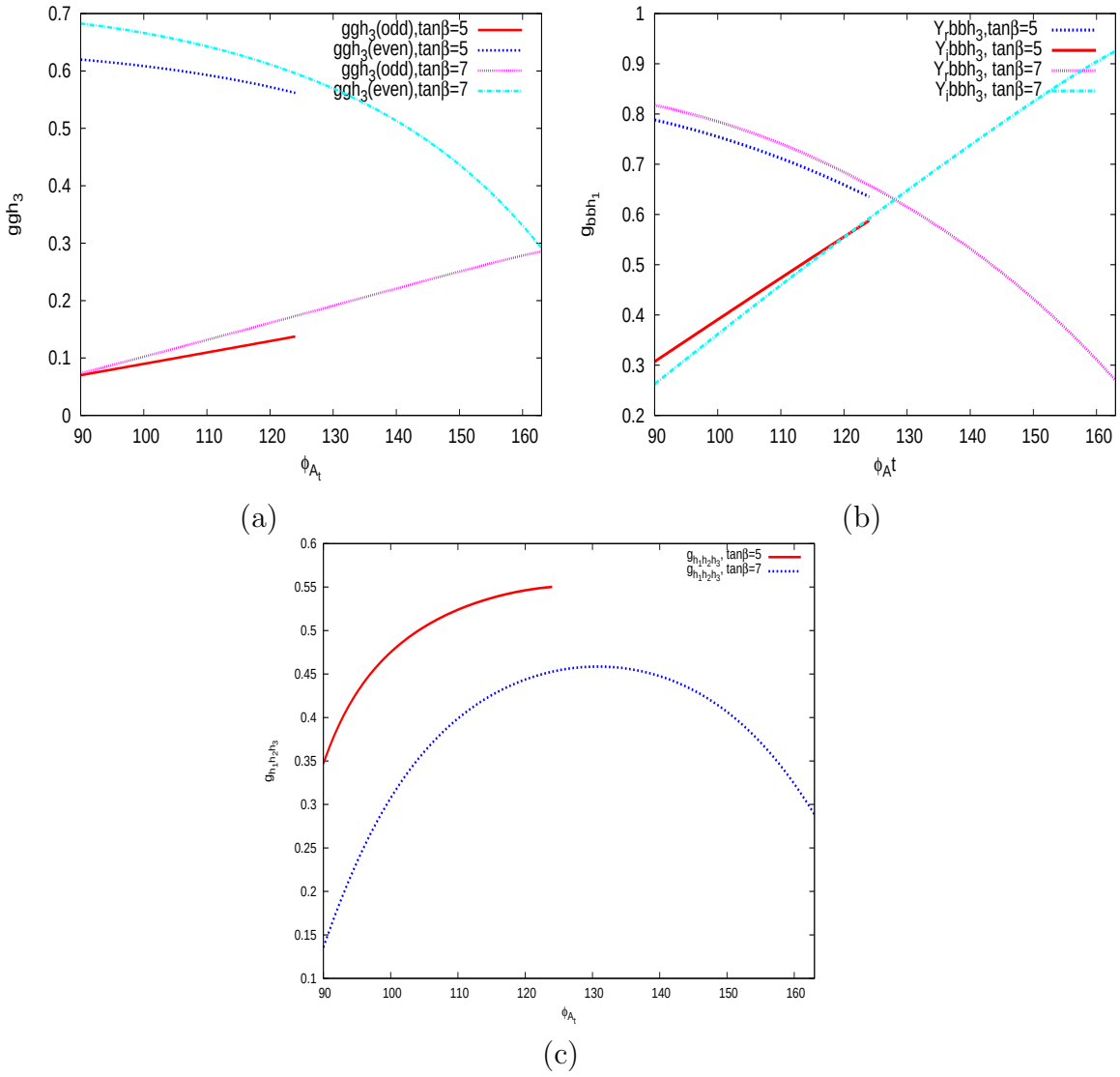

Figure 8: Variation of even and odd part of $g - g - h_3$ (upper left), y_{bbh_3} (upper right) and $h_1 - h_2 - h_3$(below) coupling vs ϕ_{A_t}. For $\tan\beta = 5$ the figures are numerically restricted to values $\phi_{A_t} \leq 124°$. [23].

No.	Final state topology	Signal BP4	Background $t\bar{t}Z$	Significance at 1 fb^{-1}	Required luminosity [fb^{-1}], 5σ significance
1	$n_{jet} \leq 4(\tau - \text{jet} \geq 3)$ $+l \geq 2(\text{OSD} \geq 1)$ $+\lvert M_{ll}\rvert \leq 2.5\text{GeV}$	1.8	0.0	1.3	14
2	$n_{jet} \leq 4(\tau - \text{jet} \geq 3)$ $+l \geq 2(\text{OSD} \geq 1)$ $+\lvert M_{ll}\rvert \leq 2.5 + \not{p}_T \leq 20$	0.6	0.0	0.77	42

Table 8: Event rates for the CPX benchmark point BP4 and background $t\bar{t}Z$ with an integrated luminosity of 1 fb^{-1}

due to the large value of ϕ_{A_t}. Figures 8(a) and 8(b) show how the odd parts of $g-g-h_3$ and $b-b-h_3$ increase as ϕ_{A_t} increases. For large ϕ_{A_t}, also $h_3 \sim h_3^{odd}$ ($h_3 = h_3^r + ih_3^{odd}$). On top of that $g_{h_3h_2h_1}$ also increases at large ϕ_{At} (see Figure 8(c)). These two effects increase $\sigma(h_1h_2)$ for large ϕ_{A_t}. Thus, for benchmark point BP3, the contribution of $\sigma(h_1h_2) = 7.93$ pb (Table 3) whereas $\sigma(h_ih_3) = 0.248$ pb, where i=1,2,3 have been included. Similarly for BP4, the contributions are $\sigma(h_1h_2) = 3.12$ pb and $\sigma(h_ih_3) = 0.464$ pb. In the case of a low ϕ_{A_t}, corresponding to BP1 and BP2; the contribution of $\sigma(h_1h_2) = 0.285, 0.323$ pb and $\sigma(h_ih_3) = 0.226, 0.206$ pb for BP1 and BP2, respectively.

4 Summary and discussion

From our analysis it is clear that the Higgs pair production is interesting in spite of being electroweak production process. We have seen that for some signal topology an integrated luminosity of 20 fb^{-1} is enough for 5σ significance. There are some points where we have a very large cross-section (BP3 and BP4) due to the enhancement of couplings. Thus, it is very easy to get discovery significance for these points. We have seen that it is also possible to reconstruct the Higgs mass peak, and we can get rid of the model backgrounds. Thus the signal topologies coming from Higgs pair productions are very different from CP-conserving case.

Production of two Higgs bosons has contribution from the subprocess including coupling of three Higgs bosons. Especially this contribution is important for our benchmark points BP3 and BP4. Since the three Higgs boson vertex comes from the Higgs potential, the production process can give information on the potential, and is thus of great interest and importance. Lastly, BP4 analysis in τ mode is relatively clean as it is background free.

Acknowledgments:

KH acknowledges support from the Academy of Finland (Project No 137960). PB wants to thank Helsinki Institute of Physics for the visit during the project and KIAS overseas travel grant. PB also thanks Prof. Jae Sik Lee for useful discussions.

References

[1] M. Dugan, B. Grinstein and L. J. Hall, Nucl. Phys. B **255** (1985) 413. S. Dimopoulos and S. D. Thomas, Nucl. Phys. B **465** (1996) 23 [arXiv:hep-ph/9510220]. Y. Kizukuri, N. Oshimo, Phys. Rev. **D46**, 3025-3033 (1992).

[2] P. Nath, Phys. Rev. Lett. **66**, 2565 (1991); Y. Kizukuri and N. Oshimo, Phys. Rev. D **46**, 3025 (1992); T. Ibrahim and P. Nath Phys. Lett. B **418**, 98 (1998); Phys. Rev. D **57**, 478 (1998); *ibid* D **58**, 019901(E) (1998); *ibid* D **60**, 079903 (1999); *ibid* D **60**, 119901 (1999); M. Brhlik, G.J. Good and G.L. Kane, Phys. Rev. D **59**, 115004 (1999); A. Bartl, T. Gajdosik, W. Porod, P. Stockinger and H. Stremnitzer, Phys. Rev. D **60**, 073003 (1999); D. Chang, W.-Y. Keung and A. Pilaftsis, Phys. Rev. Lett. **82**, 900 (1999); S. Pokorski, J. Rosiek and C.A. Savoy, Nucl. Phys. B **570**, 81 (2000); E. Accomando, R. Arnowitt and B. Dutta, Phys. Rev. D **61**, 115003 (2000); S. Abel, S. Khalil and O. Lebedev, Nucl. Phys. B **606**, 151 (2001); U. Chattopadhyay, T. Ibrahim and D.P. Roy, Phys. Rev. D **64**, 013004 (2001); D.A. Demir, M. Pospelov and A. Ritz, hep-ph/0208257.

[3] A. Pilaftsis, Nucl. Phys. B **644**, 263 (2002).

[4] T. Falk, K.A. Olive, M. Pospelov and R. Roiban, Nucl. Phys. B **60**, 3 (1999).

[5] R. Barate *et al.* [LEP Working Group for Higgs boson searches], Phys. Lett. B **565**, 61 (2003) [arXiv:hep-ex/0306033];
see also $http://lephiggs.web.cern.ch/LEPHIGGS/www/Welcome.html$

[6] S. Schael *et al.* [ALEPH Collaboration], Eur. Phys. J. C **47**, 547 (2006) [arXiv:hep-ex/0602042];
see also $http://lephiggs.web.cern.ch/LEPHIGGS/www/Welcome.html$

[7] T. Aaltonen *et al.* [CDF and D0 Collaborations], Phys. Rev. Lett. **104** (2010) 061802 [arXiv:1001.4162 [hep-ex]].

[8] See: LEP SUSY Working Group, `http://lepsusy.web.cern.ch/lepsusy`, and LEP Higgs Working Group,`LHWG-Note 2004-01`.

[9] P. Bechtle [LEP Collaboration], PoS **HEP2005**, 325 (2006) [arXiv:hep-ex/0602046].

[10] M. S. Carena, J. R. Ellis, A. Pilaftsis and C. E. M. Wagner, Phys. Lett. B **495**, 155 (2000) [arXiv:hep-ph/0009212].

[11] A. Pilaftsis, Phys. Rev. D **58**, 096010 (1998) [arXiv:hep-ph/9803297].

[12] A. Pilaftsis, Phys. Lett. B **435**, 88 (1998) [arXiv:hep-ph/9805373].

[13] M. S. Carena, J. R. Ellis, S. Mrenna, A. Pilaftsis and C. E. M. Wagner, Nucl. Phys. B **659**, 145 (2003) [arXiv:hep-ph/0211467].

[14] S. P. Das, M. Drees,
[arXiv:1010.3701 [hep-ph]]. S. P. Das, M. Drees,
[arXiv:1010.2129 [hep-ph]].

[15] E. Accomando *et al.*, [arXiv:hep-ph/0608079].

[16] P. Bandyopadhyay, [arXiv:1008.3339 [hep-ph]].

[17] Z. Li, C. S. Li and Q. Li, Phys. Rev. D **73**, 077701 (2006) [arXiv:hep-ph/0601148];

[18] P. Bandyopadhyay, A. Datta, A. Datta *et al.*, Phys. Rev. **D78** (2008) 015017. [arXiv:0710.3016 [hep-ph]].

[19] P. Bandyopadhyay, JHEP **0907** (2009) 102. [arXiv:0811.2537 [hep-ph]]; P. Bandyopadhyay, A. Datta, B. Mukhopadhyaya, Phys. Lett. **B670** (2008) 5-11. [arXiv:0806.2367 [hep-ph]]; K. Huitu, R. Kinnunen, J. Laamanen *et al.*, Eur. Phys. J. **C58** (2008) 591-608. [arXiv:0808.3094 [hep-ph]]; A. Datta, A. Djouadi, M. Guchait *et al.*, Nucl. Phys. **B681** (2004) 31-64. [hep-ph/0303095]; A. Datta, A. Djouadi, M. Guchait *et al.*, Phys. Rev. **D65** (2002) 015007. [hep-ph/0107271]; G. D. Kribs, A. Martin, T. S. Roy and M. Spannowsky, arXiv:1006.1656 [hep-ph]; G. D. Kribs, A. Martin, T. S. Roy and M. Spannowsky, Phys. Rev. D **81** (2010) 111501 [arXiv:0912.4731 [hep-ph]].

[20] D. K. Ghosh, S. Moretti, Eur. Phys. J. **C42** (2005) 341-347 [hep-ph/0412365]; D. K. Ghosh, R. M. Godbole, D. P. Roy, Phys. Lett. **B628** (2005) 131-140 [hep-ph/0412193];

A. Pilaftsis and C. E. M. Wagner, Nucl. Phys. B **553**, 3 (1999) [arXiv:hep-ph/9902371]; D. A. Demir, Phys. Rev. D **60**, 055006 (1999) [arXiv:hep-ph/9901389]; S. Y. Choi, M. Drees and J. S. Lee, Phys. Lett. B **481**, 57 (2000) [arXiv:hep-ph/0002287]; G. L. Kane and L. T. Wang, Phys. Lett. B **488**, 383 (2000) [arXiv:hep-ph/0003198]; S. Y. Choi, K. Hagiwara and J. S. Lee, Phys. Rev. D **64**, 032004 (2001) [arXiv:hep-ph/0103294]; S. Y. Choi, K. Hagiwara and J. S. Lee, Phys. Lett. B **529**, 212 (2002) [arXiv:hep-ph/0110138]; S. Heinemeyer, Eur. Phys. J. C **22**, 521 (2001) [arXiv:hep-ph/0108059]; T. Ibrahim and P. Nath, Phys. Rev. D **66**, 015005 (2002) [arXiv:hep-ph/0204092]; S. W. Ham, S. K. Oh, E. J. Yoo, C. M. Kim and D. Son, Phys. Rev. D **68**, 055003 (2003) [arXiv:hep-ph/0205244]. J. S. Lee, AIP Conf. Proc. **1078** (2009) 36 [arXiv:0808.2014 [hep-ph]].

[21] A. Pukhov, "CalcHEP 3.2: MSSM, structure functions, event generation, batchs, and generation of matrix elements for other packages", [arXiv:hep-ph/0412191].

[22] J. R. Ellis, J. S. Lee and A. Pilaftsis, Mod. Phys. Lett. A **21**, 1405 (2006) [arXiv:hep-ph/0605288].

[23] J. S. Lee, A. Pilaftsis, M. S. Carena, S. Y. Choi, M. Drees, J. R. Ellis and C. E. M. Wagner, Comput. Phys. Commun. **156**, 283 (2004) [arXiv:hep-ph/0307377]. J. S. Lee, M. Carena, J. Ellis, A. Pilaftsis, C. E. M. Wagner, Comput. Phys. Commun. **180**, 312-331 (2009). [arXiv:0712.2360 [hep-ph]].

[24] H. L. Lai *et al.* [CTEQ Collaboration], Eur. Phys. J. C **12**, 375 (2000) [arXiv:hep-ph/9903282].

[25] J. Pumplin, D. R. Stump, J. Huston, H. L. Lai, P. Nadolsky and W. K. Tung, JHEP **0207**, 012 (2002) [arXiv:hep-ph/0201195].

[26] T. Sjostrand, L. Lonnblad and S. Mrenna, [arXiv:hep-ph/0108264].

[27] See "http://hep.pa.msu.edu/people/belyaev/public/calchep/index.html"

[28] P. Skands *et al.*, JHEP **0407**, 036 (2004) [arXiv:hep-ph/0311123]; see also $http://home.fnal.gov/\tilde{}skands/slha/$

[29] H. Baer, V. Barger, G. Shaughnessy, H. Summy and L. t. Wang, Phys. Rev. D **75**, 095010 (2007) [arXiv:hep-ph/0703289].

[30] M. Frank, T. Hahn, S. Heinemeyer, W. Hollik, H. Rzehak and G. Weiglein, JHEP **0702**, 047 (2007) [arXiv:hep-ph/0611326].

[31] T. Hahn, S. Heinemeyer, W. Hollik, H. Rzehak, G. Weiglein and K. Williams, [arXiv:hep-ph/0611373].

[32] G. L. Bayatian *et al.* [CMS Collaboration], J. Phys. G **G34** (2007) 995-1579.

[33] G. Bagliesi, [arXiv:0707.0928 [hep-ex]].